SSRG International Journal of Electronics and Communication Engineering
ISSN: 2348-8549/ https://doi.org/10.14445/23488549/IJECE-V10I8P112

Volume 10 Issue 8, 118-127, August 2023

Original Article

Fuzzy Refinement-Based Tissue and Ring Connectivity for Brain Skull Segmentation

Nisha Bernad Singh[1], Victor Jose Marianthiran[2]

[1]*Department of Computer Application, Noorul Islam Centre for Higher Education, Kumaracoil, Kanyakumari, Tamilnadu, India.*
[2]*Department of Computer Science and Engineering, Vel Tech Multi Tech Dr. Rangarajan Dr. Sakunthala Engineering College, Chennai, Tamilnadu, India.*

[1]*Corresponding Author : n4230501@gmail.com*

Received: 19 June 2023 Revised: 20 July 2023 Accepted: 16 August 2023 Published: 31 August 2023

Abstract *- Magnetic Resonance Imaging (MRI) based brain cancer segmentation methods need the skull stripping algorithms as their pre-processing tool. Skull stripping is challenged by less accuracy and high time consumption; hence, an effective skull stripping method is needed for the medical world. In this research, a novel skull stripping method on brain MRI is proposed, which is named 'Skull Stripping in brain MRI using FHECE based enhancement, Fuzzy clustering and Morphological operations (SS_FFM)'. The contribution of this paper is the 'Fusion of Histogram Equalization and Edge-based Contrast Enhancement (FHECE)'. The proposed SS_FFM method essentially segments the brain tissue region from the background and skull region of brain MRI. The FHECE method enhances the brain MRI using the novel approach of weighted fusion of Adaptive Histogram Equalization (AHE) and edge-based contrast enhancement. The proposed SS_FFM method is also empowered by a new concept, which is an integrated component based on the three binary clustered outputs along with the 'Tissue and skull ring connectivity detection'. The main advantage of this paper is the independent skull stripping against the 'Tissue and skull ring connectivity' characteristic. Segmentation Accuracy (SA) analysis reveals that the proposed SS_FFM method enhances the SA by 1.39% compared to the second-best method. The proposed method reduces the time consumption by 46.19% compared to the second-best SS-UNET method. Experimental results in terms of F Score and Segmentation accuracy prove the extended efficiency of the proposed method. Hence, it can be used as a tool for medical practitioners.*

Keywords *- Brain skull segmentation, Fuzzy c means, MRI tissue region separation, MRI enhancement, Medical image processing.*

1. Introduction

Magnetic Resonance Imaging (MRI) is an advanced imaging technique in the medical field. MRI produces high-quality images of various internal human body organs, including the brain, tissues, and so on [1, 2]. The MRI scan is used to detect the presence of a brain tumor. Magnetic Resonance Imaging (MRI) is the most common and preferred diagnostic mode for detecting brain tumors.

Brain cancer is the main cause of cancer deaths, which residue a severe health threat and is mostly not curable. The beginning stage of brain cancer can be diagnosed accurately for disease management. Brain cancer symptoms are headache, nausea, seizure, or central neurological impairments emerge [3]. The brain cancer includes gliomas, meningiomas, and pituitary tumors.

Skull stripping is the beginning step in the path of identifying abnormalities in the brain. Brain extraction is the process of eliminating the skull and non-brain tissues from brain MRI scans. The non-brain tissues include skin, neck, muscle, and eyeballs. In automatic brain tumor segmentation, the main complication is the occurrence of non-brain tissues; hence, skull stripping is much needed. The existing skull segmentation methods are manual segmentation, intensity-based segmentation, atlas-based segmentation, surface-based segmentation, and hybrid segmentation [4, 5]. The brain images are acquired using different imaging limits on machines with different scan quality. The various brain structures have the same signal intensities, which often overlap. Domain-specific knowledge is needed for skull stripping. The challenge is on large datasets [4-7].

The existing methods of skull stripping have less accuracy and less speed. The echoes can be seen in the tissue borders of brain images [6, 7], making small links connecting the skull and tissue regions. Major methods fail to eliminate the skull region that touches the tissue region. Hence, there is

a need for the new development in skull stripping in brain MRI images. The aforementioned issues motivated this research to propose a new method for skull stripping entitled 'Skull Stripping in brain MRI using FHECE based enhancement, Fuzzy clustering and Morphological operations (SS_FFM)'. The contributions set with the proposed method are:

- A new brain MRI image enhancement algorithm is described, namely 'Fusion of Histogram equalization and Edge-based Contrast Enhancement (FHECE).'
- A new mechanism to detect the connectivity/attached status of skull and tissue region
- Two individual essential techniques to attach and detach the status of skull and tissue regions using binary images of Fuzzy C Means (FCM) segmentation.

In this work, the input is a noise-removed grayscale MRI brain image, and the result is a skull-removed image that includes the brain's tissue region.

Section 2 explains the related works done in skull stripping. Section 3 describes the working methodology of the proposed method. Section 4 explains the discussion and analysis of the proposed skull stripping method with various analytic measures. Section 5 describes the conclusion of the analysis part.

2. Related Works

Faisan et al. [8] described an atlas-based method for skull segmentation. This method warps a binary image. The disadvantage is that there are theoretical problems with label image topology. Park et al. [9] described a cranial dissection method based on regional growth in MRI images. The downside is the erroneous transmission due to the masking operation. Somasundaram et al. [10] referred to a hybrid method for skull segmentation. The hybrid method combines the mean filter and the image contour detection algorithm. The disadvantage is the label variation in segmentation for the same intensity values. Liu et al. [11] depicted a clustering application for tissue segmentation. This algorithm segments the brain MRI data. Also, it exploits the feature and spatial information in the data. The drawback is that it is difficult to brain image segmentation without prior information. Payam et al. [12] put forth an approach for symmetric segmentation of three-dimensional objects. The weakness of this method is that the symmetric interaction reduces the dependency on the initialized methods. Iglesias et al. [13] described an agreement-based skull-stripping method. The framework is used to test unlabeled data. The demerit of this semi-supervised algorithm is the unsuitableness for the bulk of scans.

Wang et al. [14] explained a deformable surface-based method for skull segmentation. The deformable surface-based method for skull-stripping uses a bulky number of images with the constraint setting. The disadvantage is that the less consistent outcome is generated for a fixed constraint. Speier et al. [15] depicted a skull segmentation technique for clinical data. Weakness is that it is incapable of walking around all the directions in the brain skull. Zhou et al. [16] described a method for skull segmentation using a vector machine-based technique. The method plans to create an online hybrid support vector classifier. The disadvantage is that the ending segmentation results have a high false rate. Uher et al. [17] described a 3D brain tissue segmentation method. This is a completely automatic process that evaluates brain tissue size using MRI scans. The Statistical region merging function is used for 3D image segmentation. For each segment, the factors are calculated. The drawback is that it can be applied only to U-Net architecture. Kalavathi [18] demonstrated a technique using multiple Otsu's thresholding technique for tissue segmentation. This technique chooses an optimal threshold value that supports segmenting WM, GM and CSF from MRI brain images.

Otsu's thresholding technique has the drawback of being used to test a small volume of brain images. Lv et al. [20] referred to a surface-based method for T1-weighted images. This method works based on an integrated segmentation algorithm and 3D interpolation. The drawback is that the reconstruction is fast only for 3D T1-weighted MRI images. Chansuparp et al. [21] described an integrated method for skull stripping. This method is a combination of mathematical morphology and component labels. The drawback is that, in some situations, it is challenging to separate the cerebral region that curls up to the skull. A method for semi-supervised discriminative classification of MR brain images. The drawback is that tumor segmentation is difficult for huge data sizes.

3. Proposed Methodology

This paper proposes a new skull segmentation approach, namely SS_FFM. The main contribution of this paper is the FHECE algorithm that tunes the brain MRI image in an enhanced form with better contrast distribution. Another new procedure is proposed, a joined work on the three binary clustered outputs along with the 'skull and tissue inter-connectivity detection'. Morphological operations are utilized to make skull stripping in MRI. Figure 1 depicts the overall work of the proposed SS_FFM approach. MRI brain image in the format of grayscale having the size of 512x512 is fed as input to the proposed method. The output image is the skull-stripped version, which consists only of the tissue region. Figure 2 reveals the building blocks of the proposed method in a detailed model. The proposed work is divided into four divisions:

- FHECE-based MRI image enhancement
- Segmentation using Fuzzy logic
- Optimum segmented binary image detection
- Tissue segmentation technique.

MRI brain images are normally set with highly varying contrast, and their edges are not much defined so that the edges between the skull and tissue region are not much exposed, which leverages the failure ratio in skull segmentation. Hence, the MRI brain images must be enhanced for a clear visual.

3.1. FHECE-Based MRI Image Enhancement

This research designs a new step to enhance the contrast of the skull area of MRI images, namely FHECE. It contains the following three steps to do the enhancement:

- Adaptive Histogram Equalization (AHE)
- Edge-aware local contrast enhancement
- Weighted Fusion of AHE and Edge-based contrast enhancement.

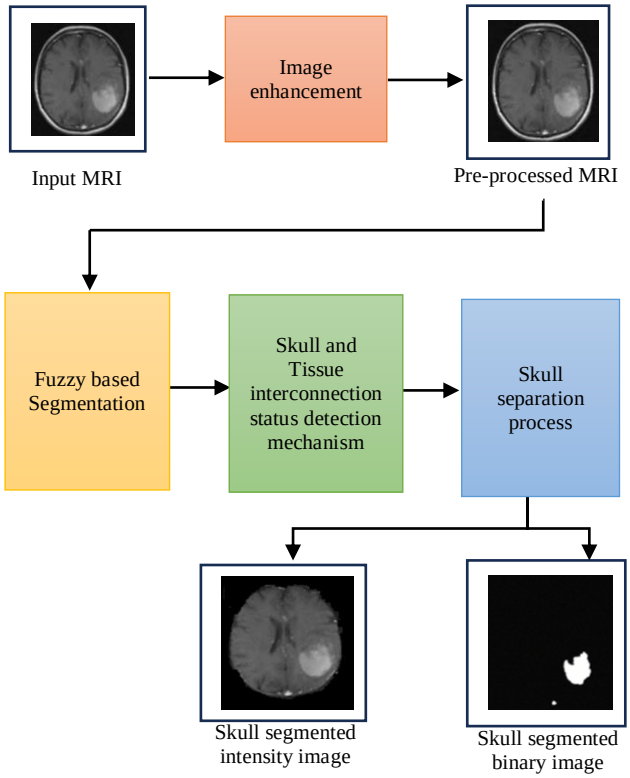

Fig. 1 Overall diagram for the proposed SS_FFM approach

Brain MRI image IP is set as input to the AHE and processes the histogram equalization separately to every small block. Figure 3(a) shows the input image. The built-in function of MATLAB, namely adapthisteq (), is applied here to get the AHE enhancement. The contrast-improved resultant image is noted as I_AHE and shown in Figure 3(b). This image lightens the less contrast regions; hence, the skull-ring region is brightened. This action differentiates the skull-ring region from both tissue and background regions.

With the aid of the local mean and standard deviation calculations for each pixel, the Edge Aware Local Contrast (EALC) enhancement enhances contrast based on edge locations. Additionally, it adjusts the values of the pixels in accordance with the derived statistics.

Here, the standard deviation algorithm type, window size, and contrast gain factor are utilized to estimate the values of the pixels depending on the pixels around them. The EALC is implemented using the built-in function named 'localcontrast()' of MATLAB, which is tuned by assigning the edge_threshold=0.4 and amount=0.001. The resultant enhanced image is noted as I_EALC and shown in Fig.3(c). In this output, a flattening process is applied by smoothing data while leaving strong edges unaltered.

In Figure 3(c), the general brightness is maintained, and the variations in grey levels are better levelled. The minimum intensity amplitude of the strong edge is pointed out by the edge_threshold parameter, while the 'amount' notifies the smoothing amount.

Weighted fusion technique is employed using both the I_AHEimage and the I_EALCimage to obtain an enhanced clarity image version, which obeys the subjective improvement, using Equation (1).

$$I_{FUSE}^{i,j} = W_{AHE} * I_{AHE}^{i,j} + W_{EALC} * I_{EALC}^{i,j} \quad (1)$$

$$i \in [0, H-1], j \in [0, W-1]$$

In Equation (1), the term I_FUSE refers to the 'enhanced image by fusion', W_AHE refers the weight value related to AHE (let it be 0.34), W_EALC refers to the weight related to EALC output (let it be 0.66), H refers the height of the image and W refers the width of the image. Herein, both weights' integrated weight values are exclusively fixed as 1. The brain skull region benefits from the equalized output from I_AHE and the stabilized output from I_EALC. Figure 3(d) shows the final enhanced fused MRI that highlights the ring-type skull borders than the others, and the other benefit is that it does not possess over-enhancement and under-enhancement. Another essential gain is that the skull borders are defined visually better than the input image, which aids in having a better skull stripping output.

3.2. Fuzzy Based Segmentation

A notion called fuzzy logic is used to support information that is unclear or imprecise. Unlike the binary system, the fuzzy logic membership degree is set from completely false to completely true. The fuzziness range is configured to be between 0 and 1. The Fuzzy C Means (FCM) method clusters an image or segment an MRI image by assigning each data point to a cluster head based on its similarity to other points in the same cluster via the soft assignment.

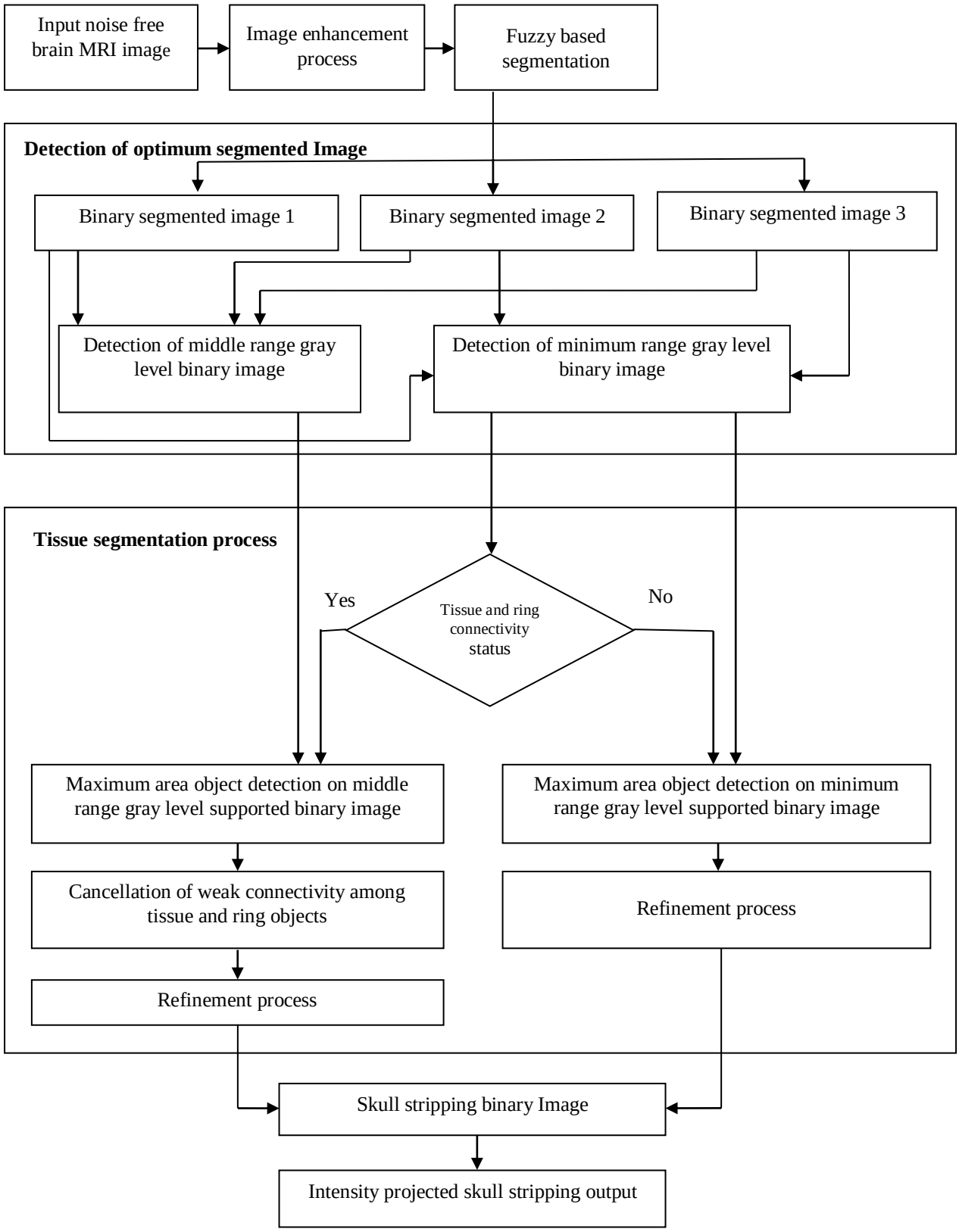

Fig. 2 Basic building blocks of the proposed SS_FFM method

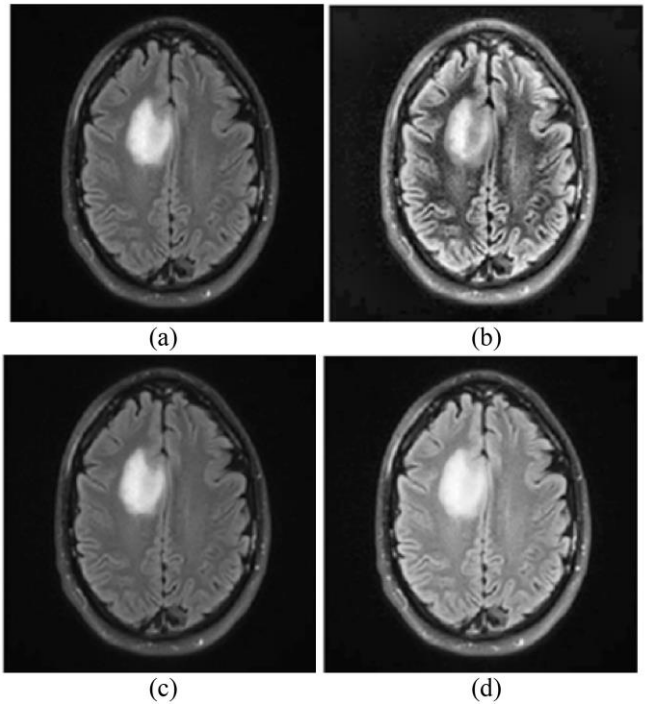

Fig. 3 Demonstration of proposed FHECE-based enhancement, (a) input MRI, (b) AHE output, (c) edge-aware contrast enhancement, (d) Final FHECE-based skull region enhancement

The I_FUSE image is the input to the fuzzy segmentation process. In the initialization stage of FCM, the 2D image data is converted into 1D linear vector X that sets with the length corresponding to H * W. Because there are three different types of regions in the MRI image, viz. the background, skull, and tissue, the Total clusters h is set to 3 in this instance. Herein, Membership matrix U_(i,j) is randomly settled, vector length l is fixed as H *W, maximum iteration p is set to 100, error level e is set to 0.001, and the exponent term q is set to 2. The array of cluster heads is noted by C_j, where j is the cluster index. FCM method clusters the MRI based on equations from Equation (2) to Equation (4).

$$C_j = \frac{\sum_{i=0}^{n-1}(U_{i,j})^q \times X_i}{\sum_{i=0}^{n} U_{i,j}}, j \in [0, h-1] \quad (2)$$

$$d_{i,j} = |X_i - C_j|, \quad (3)$$

$$j \in [0, h-1], i \in [0, H*W-1]$$

$$U_{i,j} = \begin{cases} \sum_{t=0}^{n-1} \left(\frac{d_{i,j}}{d_{i,t}}\right)^{\frac{2}{q-1}}, if\ d_{i,j} \geq 0 \\ 1, \quad else \end{cases} \quad (4)$$

Herein, Cluster head C_j is computed using Equation (2), the distance d_(i,j) is computed using Equation (3), and the membership value is calculated using Equation (4). High similar data points hold higher membership values towards the related cluster head than dissimilar cluster heads. The objective function finds out the convergence level of iteration using the error level e.

3.3. Optimum Segmented Binary Image Detection

Due to the fact that there are three clusters, or the image comprises three binary images, the FCM output image is labelled with three distinct values, such as 1, 2, and 3. The main goal of this work is to select the most supportive binary image out of the three images that correspond to the tissue item.

The first binary image corresponding to the label 1 is extracted from the I_FCM image using Equation (5).

$$I_{BIN1}^{i,j} = \begin{cases} 1, if\ I_{FCM}^{i,j} = 1 \\ 0, else \end{cases} \quad (5)$$
$$\in [0, IH-1], j \in [0, IW-1]$$

Herein, the terms I_BIN1^(i,j) refer to the binary image based on label 1. Equation (5) focuses the background by a value of 0, while the foreground object is focused by a value of 1. The second binary image I_BIN2^(i,j) in the same model can be created using the label value 2 from the I_FCM image. The third binary image, I_BIN3^(i,j), is generated via the I_FCM image using a label value of 3. In the I_BIN1 image, the tissue region is exposed in a highly varying form, and in the I_BIN2 image, the tissue region is exposed as a texture form with many holes and blank spaces. However, the I_BIN3 image consists of only the skull and background regions. Here, the tissue region is exposed through the pixels that are represented by zeros. The concealed tissue region is similarly evenly dispersed with only a few foreign objects and holes. The aforementioned characteristics of the I_BIN3 picture can help to promote a highly confident tissue region detection. The unique characteristic of the I_BIN3 is that it produces less intensity than the other two binary images, namely I_BIN1 and I_BIN2.

The mean intensity μ_1 related to the I_(BIN1) image is computed using Equation (6) and Equation (7).

$$\in [0, IH-1], j \in [0, IW-1] \quad (6)$$

$$(x,y) = \begin{cases} y, if\ x = 1 \\ 0, else \end{cases} \quad (7)$$

$$i \in [0, H-1], j \in [0, W-1]$$

Herein, the term $f(x,y)$ refers to the function to compute the eligibility of the pixel to participate in the μ_1 calculations and FC_1 refers to the Foreground pixel count in I_{BIN1} image. In the same model, the mean intensity μ_2 related

to I_{BIN2} image is computed. Also, the mean intensity μ_3 related to I_{BIN3} is computed. The tissue region's highly supported binary image consistently yields the lowest mean value. This rationale is based on the idea that a binary image supported by a tissue region will always have a large number of zeros in the tissue regions and a large number of ones in the background and skull regions. This circumstance results in the lowest intensity because the background data range is constantly very close to the intensity value of zero. Thus, the mean value is drastically decreased. The minimum mean value μ is found among the three mean values, such as μ_1, μ_2 and μ_3.

3.4. Fuzzy Based Segmentation

By identifying the largest object in the "Minimum range grey level binary image," namely I_{BMIN}, this section employs a novel model to determine connectivity between the ring structure and the tissue region. The I_{BMIN} the image presents the tissue region by zeros. The ring-connectivity-status detection algorithm requires the tissue representation by $1s$; hence, the I_{BMIN} image is converted to the 'inverted form I_{INV}' using Equation (8) by subtracting each pixel by 1.

$$I_{INV}^{i,j} = 1 - I_{BMIN}^{i,j} \quad (8)$$
$$i \in [0, IH-1], j \in [0, IW-1]$$

At present, the tissue region is depicted by 1s rather than 0s. The inverted image I_INV. The whole connected components of the I_INV image are found, and the area property of each of them is calculated. Afterwards, the maximum area providing the connected component is found using morphological operations and stored in an individual binary image I_BIG. The subtraction process between the I_INV and I_BIG images reveals that the difference is high for the disconnected ring object while it is less for the connected ring object model. The subtracted binary image is noted as I_SUB^(i,j).

Because the geometry of the largest component is nearly identical to the foreground object of I_INV, the I_INV image and the I_BIG image cancel each other out in major pixels when applied to the connected skull model. The subtracted image I_SUB contains the skull object since it has more values of 1s than the threshold in the disconnected skull model, which cancels only the tissue region and not the skull region. Simply said, the I_SUB image for a connected model has fewer 1s than the threshold th, whereas the I_SUB image for a disconnected model has more 1s than the threshold th. The skull-connected status SCS is detected via Equation (9) and Equation (10).

$$S = \sum_{i=0}^{IH-1} \sum_{j=0}^{IW-1} I_{SUB}^{i,j} \quad (9)$$

$$SCS = \begin{cases} 1, & if\ S \le th \\ 0, & else \end{cases} \quad (10)$$

Equation (9) computes the sum of all 1s in the I_SUB image and sets it in S. Equation (10) sets 1 in SCS for the skull-connected status and sets 0 for skull disconnected status. The tissue separation process is expressed using two cases. They are:

Skull and tissue disconnected model (i.e., case 1)
Skull and tissue connected model (i.e., case 2).

3.4.1. Case 1: (Skull & Tissue Disconnected Model)

The largest object image, I_BIG, already represents the tissue region. Thus, no additional steps are required to segment the tissue region if the skull's connected status is zero. It needs only the following pre-processing steps to leverage the tissue section's segmentation quality.

Morphological filling process.
Morphological hole-filling process.
Morphological closing process.
Morphological background filling process.

Morphological filling is employed in the image I_BIG to fill the isolated interior pixels, and the output is noted as I_MF, which is shown in Figure 4(d). The I_MF image has undergone the morphological hole-filling process to fill the holes, eliminating the island-like structures in the tissue region. The output is noted as I_MH and shown in Figure 4(e). The morphological closing operation is progressed in the I_MH image to reduce the size of small background objects while maintaining the overall shape of the larger foreground objects. The 'disk' type structuring element with 3 length diameter is utilized here to apply the closing operation. The output is noted as I_MC and shown in Figure 5(f). Morphological filling is employed over the image I_MC to fill the background data by 1s. The background-filled image is noted as I_BF, and shown in Figure 5(g) shows the background-filled image.

3.4.2. Case 2: (Skull & Tissue Connected Model)

The middle range gray level binary image I_BMID is utilized here to separate the tissue region. The biggest object in the I_BMID image is found and stored as I_BIG. Assume a pixel [i,j] in the I_BIG image, and afterwards, a sequence of ten pixels in the left direction is taken out using Equation (11).

$$ARR_{LEFT}^{K} = I_{BIG}^{i,j-K}, K \in [0,9] \quad (11)$$

In Equation (10), the term ARR_{LEFT} means the Left directional sequence of 10 pixels. The summing process is applied in ARR_{LEFT} array, and the result is stored as SUM_{LEFT}. The sequence of 10 pixels in the right direction is found using Equation (12).

$$ARR_{RIGHT}^{K} = I_{BIG}^{i,j+K}, K \in [0,9] \quad (12)$$

The summing process is applied in ARR_{RIGHT}^{K} array, and the results are stored as SUM_{RIGHT}. The sequence of 10 pixels in the top direction is found using Equation (13).

$$ARR_{Top}^{K} = I_{BIG}^{i-K,j}, K \in [0,9] \quad (13)$$

The summing process is applied in ARR_{Top}^{K} array, and the results are stored as SUM_{TOP}. The sequence of 10 pixels in the bottom direction is found using Equation (14).

$$ARR_{BOTT}^{K} = I_{BIG}^{i+K,j} \ , \ K \in [0,9] \quad (14)$$

The summing process is applied in ARR_{BOTT}^{K} array, and the results are stored as SUM_{BOTT}.

The corresponding $[i,j]^{th}$pixel is considered the "connected pixel" in the course of the connective line of the skull and tissue if any of the four "sum oriented data" in any direction is less than the threshold value of 4. As a result, that pixel is changed to 0, which signifies the elimination of the connection between the tissue region and the skull. It can be described using Equation (15).

$$I_{BIG}^{i,j} = \begin{cases} 0, if\ SUM_{LEFT} < 4 || SUM_{RIGHT} < 4 \mid \\ \quad SUM_{RIGHT} < 4 \mid SUM_{BOTT} < 4 \\ I_{BIG}^{i,j},\ els \end{cases} \quad (15)$$

The connection between the skull and tissue region is cut off during the entire procedure that corresponds to every single pixel. Afterwards, the connection-eliminated I_BIG image is processed by morphological operations such as image filling, holes filling, closing operation and background filling to refine the tissue image.

The connection between the skull and tissue region is cut off during the entire procedure, corresponding to every pixel. Afterwards, the connection-eliminated I_BIG image is processed by morphological operations such as image filling, holes filling, closing operation and background filling to refine the tissue image.

3.5. Skull Removal Process

Equation (16)'s *adding* procedure is used to combine two images, such as I_{MC} and I_{BF} to create the binary tissue segmented image I_{BTS}.

$$I_{BTS}^{i,j} = \begin{cases} 1, if\ (I_{MC}^{i,j} + (1 - I_{BF}^{i,j})) > 0 \\ 0, else \end{cases} \quad (16)$$

In Equation (15), the term '$1 - I_{BF}$'means the inverted form of I_{BF} image. The adder image I_{BTS} is the final enhanced skull removed from the image.

Equation (17) is used to create the final "intensity projected tissue segmented image" by projecting the input image's intensity information onto the I_{BTS} image's places of 1s.

$$I_{TS}^{i,j} = \begin{cases} IP^{i,j},\ if\ I_{BTS}^{i,j} = 1 \\ 0, \quad else \end{cases} \quad (17)$$

In Equation (17), the term I_{TS} refers to the tissue-segmented intensity image. Here, the intensity of the IP image is used to fill the tissue region, while zeros are used to fill the other spaces. Figure 5(h) and Figure 5(i) respectively exhibit the I_{BTS} and I_{TS} images. Thus, the proposed SS-FFM approach successfully makes the skull stripping process.

4. Discussion and Analysis

The proposed SS_FFM approach is analyzed using the three databases such as Kaggle Brain Tumor Image Dataset (KBTD_DS), Brain Images of Tumors for Evaluation Dataset (BITE_DS), and Figshare Brain Tumor Dataset (FBTD_DS). Figure 4 shows the sample images from the three databases. The first row in Figure 4 demonstrates the FBTD_DS database samples, the second row shows the BITE_DS database samples, and the third row depicts the KBTD_DS database samples.

The three existing approaches listed below are used for analysis purposes.

- Morphological Image Processing based Skull Stripping (SS_MIP)
- Multistable Cellular Neural Networks based Skull Stripping (SS_MCNN)
- 3D U-Net based Skull Stripping (SS_UNET).

Mean Square Error (MSE) analysis is used to assess the effectiveness of the proposed SS_FFM skull stripping procedure. By computing the error values, it evaluates the homogeneity property between the segmented and actual skull areas.

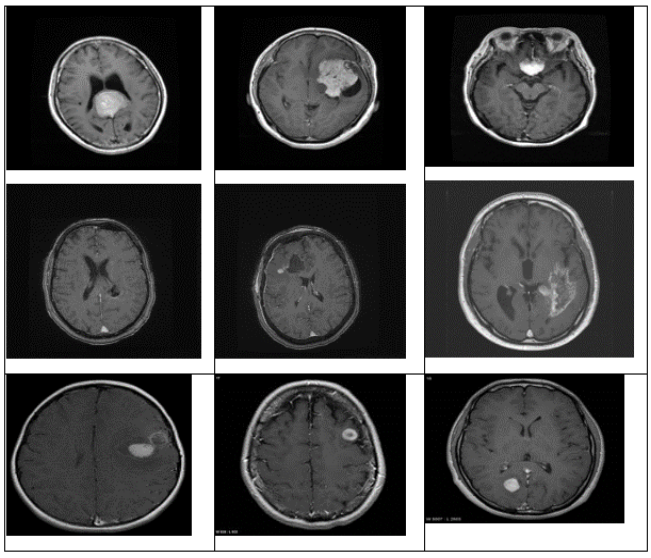

Fig. 4 Demonstration of sample database images

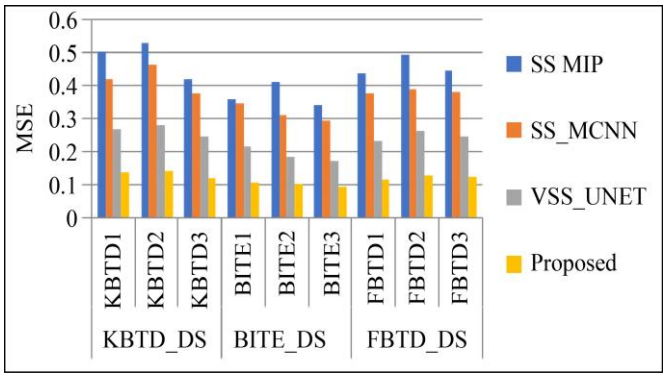

Fig. 5 Mean Square Error (MSE) analysis chart

The three existing approaches listed below are used for analysis purposes.

- Morphological Image Processing based Skull Stripping (SS_MIP)
- Multistable Cellular Neural Networks based Skull Stripping (SS_MCNN)
- 3D U-Net based Skull Stripping (SS_UNET).

Mean Square Error (MSE) analysis is used to assess the effectiveness of the proposed SS_FFM skull stripping procedure. By computing the error values, it evaluates the homogeneity property between the segmented and actual skull areas.

Figure 5 shows the MSE analysis results. The average MSE of SS_MIP, SS_MCNN, SS_UNET and the proposed methods are 0.4380, 0.3719, 0.2329 and 0.1182. The proposed SS_FFM method provides a lower MSE value of 0.1182. Hence, it is declared the best skull-stripping method for the existing versions. The proposed method yields the lowest MSE value of 0.0934 for the BITE_DS database; therefore, the BITE_DS database is called the best supportive database for skull stripping.

The FScore is a metric used for evaluating the effectiveness of image segmentation. FScore measure is influenced by the two parameters, Precision and Recall.

Table 1. FScore analysis for skull segmentation

Data base	Image	FScore			
		SS_ MIP	SS_ MCNN	SS_ UNET	Pro posed
KBTD _DS	KBTD1	0.932	0.948	0.963	0.974
	KBTD2	0.930	0.944	0.961	0.971
	KBTD3	0.931	0.946	0.962	0.973
BITE _DS	BITE1	0.931	0.947	0.962	0.974
	BITE2	0.932	0.948	0.964	0.976
	BITE3	0.933	0.949	0.965	0.977
FBTD _DS	FBTD1	0.929	0.944	0.961	0.973
	FBTD2	0.928	0.942	0.960	0.971
	FBTD3	0.930	0.945	0.962	0.975

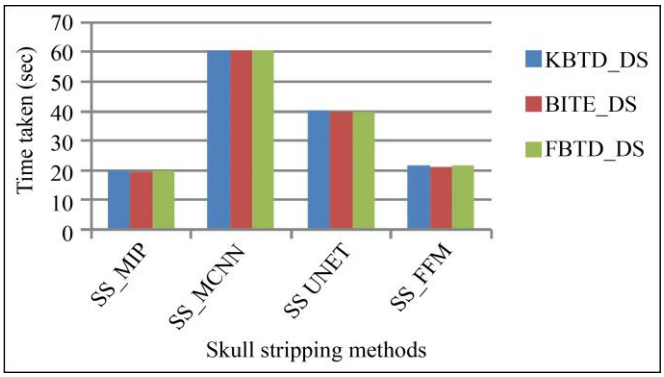

Fig. 6 Time-taken analysis

Table 1 shows the FScore analysis for skull segmentation. The proposed SS_FFM method has the highest FScore value of 0.977 for the BITE_DS database. It proves the efficiency of the proposed method than the existing method. The average FScore values of the databases like KBTD_DS, BITE_DS and FBTD_DS corresponding to the proposed method are 0.9731, 0.9760 and 0.9734. This analysis ranks the BITE_DS database as the best supportive database, and it ranks the FBTD_DS database as the secondary best database. Time Taken (TT) analysis is depicted in Figure 6. This analysis is done based on 100 test images from each database.

The proposed approach consumes less time when compared to the SS_MCNN and SS_UNET approaches. It consumes a little higher point in time than the least performance method, namely SS_MIP. However, the performance of the proposed method is much higher than the SS_MIP. Hence, the tiny time variation between the proposed and SS_MIP methods can be thought of as an acceptable one. Therefore, it can be spelt that the proposed SS_FFM method absorbs a reasonable time for skull segmentation. The overall time consumption of the proposed approach is 21.5 sec; meanwhile, the next-best method, namely SS-UNET, occupies 39.96 sec for segmenting the skull region. The proposed method reduces the time consumption by 46.19% compared to the second-best SS-UNET method.

The PSNR metric determines the similarity between the segmented and ground-truth images.

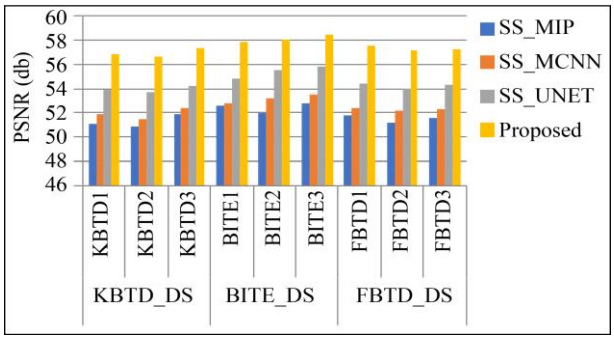

Fig. 7 PSNR analysis chart

Table 2. Segmentation Accuracy analysis

Methods	Segmentation Accuracy (%)		
	KBTD-DS	BITE-DS	FBTD-DS
SS_MIP	93.41	93.96	93.68
SS_MCNN	94.77	95.32	95.08
SS_UNET	96.60	97.10	96.89
SS_FFM	97.92	98.48	98.23

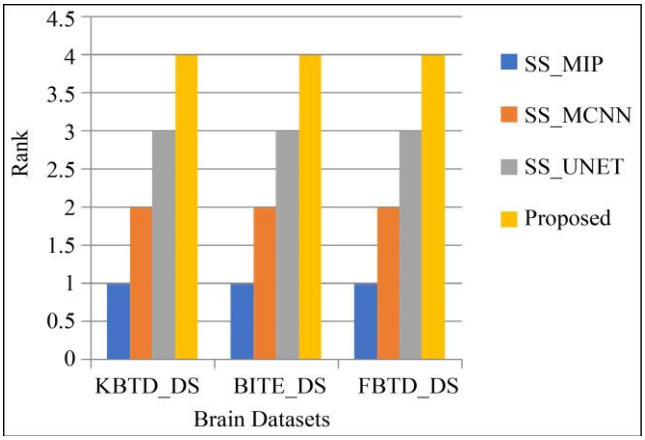

Fig. 8 Performance ranking analysis

Figure 7 depicts the PSNR analysis chart. The proposed SS_FFM method achieves the highest PSNR than the existing method. The PSNR value for the proposed SS_FFM method is 58.427 db, the highest. Average PSNR results corresponding to FBTD-DS, BITE-DS and KBTD-DS are 57.285, 58.106 and 57.081. The BITE-DS dataset is noted as the best dataset to prop up the skull-stripping methods due to its highest average PSNR value of 58.106.

The performance of skull stripping for the proposed and existing method is examined using the segmentation accuracy.

Table 2 exhibits the segmentation accuracy evaluation. The average segmentation accuracy for the proposed and SS-UNET methods is 98.21% and 96.86%; hence, the proposed approach is honored as the top, and the SS-UNET method is noted as the next-best approach. The proposed method improves the segmentation accuracy by 1.39% compared to the next-best method, namely SS-UNET.

Figure 8 shows the performance ranking analysis chart. The rank is allocated based on the performance efficiency in MSE, PSNR, FScore and segmentation accuracy. The proposed SS_FFM method is determined as the best method for skull segmentation, and therefore, it has an index value of 4.

The proposed work solves the issues of the existing methods, such as high time consumption and less accuracy. Moreover, it is a reliable work in brain skull stripping. It solves the high hardware conversion cost issue due to its less complex architecture. It also solves the tissue segmentation problem when interconnected between the skull and tissue regions.

5. Conclusion

This paper develops a new skull-stripping algorithm to segment the brain skull region of MRI images. The main contribution of this work is the FHECE algorithm, which can enhance the contrast of the brain MRI image. The proposed SS_FFM method generates top-grade performance quality in skull segmentation and robustness against scaling, accuracy, and time complexity. Standard analytic metrics prove the efficiency of the proposed method in terms of segmentation accuracy, FScore, time taken, etc. The SS_UNET method is noted as the second-best for skull segmentation. This analysis is evidence for the best support of the BITE_DS database than the other two databases. The average segmentation accuracy, FScore and time taken values for the proposed SS_FFM method are 98.21%, 0.974 and 21.5 sec, respectively, whereas those metrics for the next-best method are 96.86%, 0.962 and 39.96 sec. When compared to the existing methods, the proposed SS_FFM method is stated as the best method for tissue removal and skull segmentation.

Acknowledgments

The author would like to extend his sincere gratitude to the supervisor for his direction and unflinching support during this work.

References

[1] Muhammad Assam et al., "An Efficient Classification of MRI Brain Images," *IEEE Access*, vol. 9, pp. 33313-33322, 2021. [CrossRef] [Google Scholar] [Publisher Link]

[2] Siyabonga, and Shira, "Separation from Brain Magnetic Resonance Images (MRI) using Multistage Thresholding Technique," *SSRG International Journal of Pharmacy and Biomedical Engineering*, vol. 2, no. 3, pp. 9-13, 2015. [CrossRef] [Publisher Link]

[3] Huile Gao, and Xinguo Jiang, "Progress on the Diagnosis and Evaluation of Brain Tumors," *Cancer Imaging*, vol. 13, no. 4, pp. 466-481, 2013. [CrossRef] [Google Scholar] [Publisher Link]

[4] Ivana Despotović, Bart Goossens, and Wilfried Philips, "MRI Segmentation of the Human Brain: Challenges, Methods, and Applications," *Computational Intelligence Techniques in Medicine*, 2015. [CrossRef] [Google Scholar] [Publisher Link]

[5] Sindhia et al., "Brain Tumor Detection using MRI by Classification and Segmentation," *SSRG International Journal of Medical Science*, vol. 6, no. 3, pp. 12-14, 2019. [CrossRef] [Google Scholar] [Publisher Link]

[6] P. Kalavathi, and V.B. Prasath, "Methods on Skull Stripping of MRI Head Scan Images-A Review", *Journal of Digital Imaging*, vol. 29, no. 3, pp. 365-379, 2016. [CrossRef] [Google Scholar] [Publisher Link]

[7] P. Kanmani, P.Marikkannu, and M. Brindha, "A Medical Image Classification using ID3 Classifier," *SSRG International Journal of Computer Science and Engineering*, vol. 3, no. 10, pp. 8-11, 2016. [CrossRef] [Google Scholar] [Publisher Link]

[8] Sylvain Faisan et al., "Topology Preserving Warping of Binary Images Application to Atlas-Based Skull Segmentation," *Medical Image Computing and Computer Assisted Intervention*, vol. 5241, pp. 211-218, 2008. [CrossRef] [Google Scholar] [Publisher Link]

[9] Jong Geun Park, and Chulhee Lee, "Skull Stripping Based on Region Growing for Magnetic Resonance Brain Images," *NeuroImage*, vol. 47, no. 4, pp. 1394-1407, 2009. [CrossRef] [Google Scholar] [Publisher Link]

[10] K. Somasundaram, and P. Kalavathi, "A Hybrid Method for Automatic Skull Stripping of Magnetic Resonance Images (MRI) of Human Head Scans using Image Contour," *Second International Conference on Computing Communication and Networking Technologies*, Karur, India, pp. 1-5, 2010. [CrossRef] [Google Scholar] [Publisher Link]

[11] Jin Liu et al., "Spatially Constrained Fuzzy Hyper-Prototype Clustering with Application to Brain Tissue Segmentation," *International Conference on Bioinformatics And Biomedicine*, Hong Kong, China, pp. 397-400, 2010. [CrossRef] [Google Scholar] [Publisher Link]

[12] Payam B. Bijari et al., "Three-Dimensional Coupled-Object Segmentation using Symmetry and Tissue Type Information," *Computerized Medical Imaging and Graphics*, vol. 34, no. 3, pp. 236-249, 2010. [CrossRef] [Google Scholar] [Publisher Link]

[13] Juan Eugenio Iglesias et al., "Agreement-Based Semi-Supervised Learning for Skull Stripping," *Medical Image Computing and Computer Assisted Intervention*, vol. 6363, pp. 147–154, 2010. [CrossRef] [Google Scholar] [Publisher Link]

[14] Yaping Wang et al., "Robust Deformable-Surface-Based Skull-Stripping for Large-Scale Studies," *Medical Image Computing and Computer Assisted Intervention*, vol. 6893, pp. 635–642, 2011. [CrossRef] [Google Scholar] [Publisher Link]

[15] William Speier et al., "Robust Skull Stripping of Clinical Glioblastoma Multiforme Data," *Medical Image Computing and Computer Assisted Intervention*, vol. 6893, pp. 659-666, 2011. [CrossRef] [Google Scholar] [Publisher Link]

[16] Jiayin Zhou et al., "Segmentation of Skull Base Tumors from MRI using a Hybrid Support Vector Machine-Based Method," *Machine Learning in Medical Imaging*, vol. 7009, pp. 134-141, 2011. [CrossRef] [Google Scholar] [Publisher Link]

[17] Vaclav Uher et al., "3D Brain Tissue Selection and Segmentation from MRI," *36th International Conference on Telecommunications and Signal Processing*, Rome, Italy, pp. 839-842, 2013. [CrossRef] [Google Scholar] [Publisher Link]

[18] P. Kalavathi, "Brain Tissue Segmentation in MR Brain Images using Multiple Otsu's Thresholding Technique," *8th International Conference on Computer Science and Education*, Colombo, Sri Lanka, pp. 639-642, 2013. [CrossRef] [Google Scholar] [Publisher Link]

[19] Jaya H. Dewan et al., "Brain Tumor Type Identification from MR Images using Texture Features and Machine Learning Techniques," *International Journal of Engineering Trends and Technology*, vol. 71, no. 5, pp. 303-312, 2023. [CrossRef] [Google Scholar] [Publisher Link]

[20] Wenchao Lv et al., "Reconstruction of Brain Tissue Surface Based on Three-Dimensional T1-Weighted MRI Images," *8th International Congress on Image and Signal Processing*, Shenyang, China, pp. 481-486, 2015. [CrossRef] [Google Scholar] [Publisher Link]

[21] Manit Chansuparp et al., "The Automated Skull Stripping of Brain Magnetic Resonance Images using the Integrated Method," *8th Biomedical Engineering International Conference*, Pattaya, Thailand, pp.1-5, 2015. [CrossRef] [Google Scholar] [Publisher Link]